Catalysis Science & Technology

PERSPECTIVE

Cite this: *Catal. Sci. Technol.*, 2015, **5**, 55

Received 28th July 2014,
Accepted 8th September 2014

DOI: 10.1039/c4cy00976b

www.rsc.org/catalysis

New challenges in gold catalysis: bimetallic systems

Alberto Villa,[a] Di Wang,[b] Dang Sheng Su[cd] and Laura Prati*[a]

Since the discovery of the peculiar catalytic activity of gold catalysts, it became clear that gold could play a fundamental role also as a modifier. Indeed, more active catalysts such as those based on Pd or Pt showed specific and sometimes unexpected properties when modified with gold. This paper reviews advances in the field of Au-based bimetallic catalysts with particular attention to their preparation, characterization and catalytic activity. AuPd catalysts, the most widely studied, have been chosen as an example to show how the different obtained morphologies (alloy, core–shell, decorated particles) can contribute to the catalytic activity.

Introduction

Metal nanoparticles (NPs) have received a lot of interest in the last decade because of their unique properties, finding potential applications in different fields such us catalysis, electronics, optics, imaging, and biology.[1]

In particular over the last twenty years, gold has established an important role in the field of catalysis. Haruta and Hutchings disclosed the peculiar activity of this metal in CO oxidation and ethylene hydrochlorination.[2,3] The use of gold in catalysis has been enormously expanded,[4] however, since the beginning of its application, the use of gold for manufacturing new catalytic systems was affected by the high variation in the catalytic performances depending on the preparation method employed and the support used.[5] Indeed, many studies stated the importance of preparation

[a] *Dipartimento di Chimica, Università degli Studi di Milano, via Golgi 19, 20133 Milano, Italy. E-mail: Laura.Prati@unimi.it*
[b] *Institut für Nanotechnologie, Karlsruher Institut für Technologie, Hermann-von-Helmholtz-Platz 1, 76344 Eggenstein-Leopoldshafen, Germany*
[c] *Department of Inorganic Chemistry, Fritz Haber Institute of the Max Planck Society, Faradayweg 4–6, Berlin 14195, Germany*
[d] *Shenyang National Laboratory for Materials Science Institute of Metal Research Chinese Academy of Sciences, 72 Wenhua Road, Shenyang 110016, China*

Alberto Villa

Alberto Villa is an Assistant Professor at the University of Milan. He received his Ph.D. in Industrial Chemistry in 2007 from the University of Milan, where his thesis focused on the development of gold-based catalysts for liquid phase reactions. After two years as a PostDoc at the Fritz Haber Institute of the Max Planck Gesellschaft of Berlin, he joined Laura Prati's group in 2009. His current research focuses on the development of heterogeneous catalysts for biomass transformation. He has (co)authored over 60 publications in peer-reviewed journals.

Di Wang

Dr Di Wang received his Ph.D. in 2001 with Prof. Fanghua Li from the Institute of Physics, Chinese Academy of Sciences. From 2001 to 2009, he worked as a postdoctoral researcher with Prof. Schlögl at the Fritz Haber Institute of the Max Planck Society for TEM characterization of heterogeneous catalysts to understand the correlation between structure and catalytic behavior. Since 2009, he has worked as a research scientist at the Institute of Nanotechnology and the Karlsruhe Nano Micro Facility (KNMF), Karlsruhe Institute of Technology. His research activities are focused on using aberration-corrected HRTEM techniques, high spatially resolved EDX and EELS spectroscopy, HAADF STEM and tomography for the structural characterization of a wide range of nanomaterials, particularly supported nanocatalysts. He has (co)authored over 80 publications in peer-reviewed journals.

and support in determining the morphology of the gold particles and metal–support interactions, both able to profoundly modify the activity and/or the selectivity of the whole catalyst. Therefore, a lot of attention has been paid to the preparation of gold catalysts to assess as much as possible the relation between the support/preparation method and the characteristics of the produced materials.

Gold has shown particularly promising behavior in both selectivity and resistance to deactivation compared to Pd and Pt catalysts.[6] The durability of the catalysts currently restricts the industrial application of metal-supported catalysts, in particular, in liquid phase oxidations when dioxygen or air are used as the oxidant.[6] In addition, a serious drawback for the industrial exploitation of gold catalysts is the apparent need for the presence of a base.[7]

Bimetallic systems can overpass the latter limitation, combining the properties associated with the two constituent metals.[8] In most cases, there is a great enhancement in their specific physical and chemical properties owing to a synergistic effect. The kinetics of the reaction, the selectivity for the desired product and the durability of the catalyst have been shown to improve upon the alternative use of bimetallic species, where gold improved the performances of other metals such as Pd, Pt and Ru.[9]

The superior performance of bimetallic systems compared to monometallic counterparts has been reported for different chemical reactions, including CO oxidation[10] the selective oxidation of alcohols to aldehydes,[9,11] the direct synthesis of hydrogen peroxide,[12] the oxidation of primary C–H bonds,[13] and the transformation of biomass to fuel and chemicals.[14]

However, the nature of the synergistic effect often observed from an experimental point of view is not always completely understood from a surface science point of view, though much effort has been put into this task.[15] The reason for this lack of understanding lies in the variety of possible combinations of reactant, composition, and experimental conditions. Moreover, a lot of experimental data have been obtained with catalytic systems that were not fully characterized, leaving some doubt about their real morphology (alloy, core–shell, decoration) and homogeneity. This in turn has greatly limited the determination of a direct correlation between the structure of bimetallic systems and their catalytic properties, most times providing only single application examples.

The aim of this review is to provide a critical contribution highlighting the advances in this field with the most significant examples of use of gold-based bimetallics. Among them, AuPd catalysts are the most extensively studied. In general, bimetallic systems, according to their mixing pattern, could have the following four structural types: i) core–shell segregated nanoparticles with a shell of type A atoms covering a core of type B atoms (Fig. 1a): ii) subcluster segregated nanoparticles consisting of A and B subclusters that share a mixed interface (Fig. 1b): iii) mixed nanoalloys of two types of atoms being either ordered or solid solutions (Fig. 1c): iv) multishelled nanoparticles with layered or onion-like alternating shells (Fig. 1d).[16]

Au is miscible with Pd in all the compositions which facilitates obtaining AuPd alloys and limits segregation of the single metals. Moreover, AuPd alloys showed promising results in different catalytic applications such as alcohol and polyol oxidation, direct production of H_2O_2 from H_2 and O_2, C–C coupling and CO oxidation.[9–14] In this review, we will focus our attention on the application of AuPd systems in the

Dang Sheng Su

Dang Sheng Su completed his physics studies at Jilin University (PR China) in 1986 and his Ph.D. at the Technical University of Vienna (Austria) in 1991. He moved to the Fritz Haber Institut der Max Planck Gesellschaft as a post-doctoral worker in the Department of Electron Microscopy. After a short stay at the Hahn-Meitner Institut GmbH and the Humboldt-Universität zu Berlin (Germany), he joined the Fritz Haber Institut in 1999, where he worked on nanomaterials in heterogeneous catalysis and electron microscopy. He is now a Professor at the Institute of Metal Research, Chinese Academy of Sciences, Shenyang (PR China). His research interests are nanocarbons, nanocatalysis, chemical energy conversion and storage, and electron microscopy. He has published about 300 peer-reviewed papers, several book chapters and edited several special issues in international journals.

Laura Prati

Laura Prati has been an Associate Professor of Inorganic Chemistry at the Università degli Studi di Milano since 2001. She is a graduate in Chemistry (1983), received her specialisation in "Tecniche Analitiche per la Chimica Organica Fine" from the Politecnico of Milan in 1985 and received a Ph.D. in Industrial Chemistry in 1988. Her main interest is in catalytic hydrogenation and oxidation reactions and she has been involved in catalytic applications of gold since 1986.

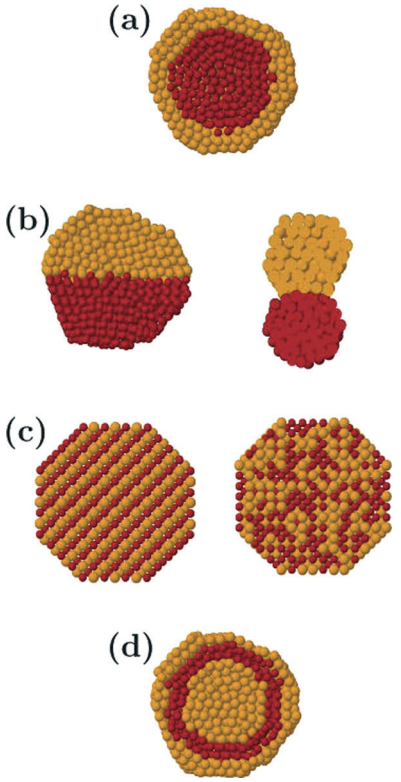

Fig. 1 Schematic representation of possible mixing patterns: core–shell (a), subcluster segregated (b), mixed (c), three-shell (d). The pictures show cross sections of the clusters. Reprinted (adapted) with permission from ref 16. Copyright (2008) American Chemical Society.

selective liquid phase benzyl alcohol oxidation and the gas-phase CO oxidation, trying to highlight the correlation between the structure and the performance of the catalyst. The first reaction plays an important role from a synthetic point of view and, when carried out as a catalytic process with O_2 as the oxidant, provides a green and sustainable alternative to the use of stoichiometric amounts of oxidant.[9] Furthermore, CO oxidation is of great importance for fundamental research as well as for applications of industrial interest such us air clean-up,[17] automotive pollution control[18] and the removal of CO traces in H_2 in fuel cells.[19] A brief survey on the available preparation methods and the characterization techniques of AuPd bimetallic systems will be provided before discussing the relationship between the structure and the catalytic performance.

Synthesis of AuPd systems

Different synthetic strategies have been proposed for the preparation of bimetallic systems. In this section we will summarize the most used ones for the preparation of gold bimetallic catalysts applied for liquid and gas phase oxidations. Among them, metal sol immobilization and the direct impregnation of metal salts are the most reported.

The first method is based on the preparation of bimetallic systems using co-reduction or consecutive reduction of metal precursors in the presence of a stabilizing agent, which passivates the nanoparticles' surface and prevents them from aggregation, and their subsequent immobilization on a support.[20] For the catalyst preparation by immobilization of metal colloids, it is very important to be able to separate the nucleation and the growth into different steps, as suggested by Lamer *et al.*[21] The reducing agent and the protective agent play a fundamental role in the structure formation of the final catalyst, being both important, for example, to tune the size of the metal nanoparticles. Normally, the use of a strong reducing agent, such as $NaBH_4$, is needed in order to simultaneously reduce both metals, but a quick metal reduction makes the nucleation and growth processes difficult to control. In such a case, the use of an appropriate protective agent can passivate the surface of the cluster making the process easier to control. Employing this strategy, it is possible, in theory, to tune the morphology of the bimetallic system. When the second metal, with a lower redox potential, is reduced, it can deposit on the surface of the preformed nucleus of the first metal symmetrically with a core–shell structure. If the two metals are completely miscible, as in the case of Au and Pd, an alloy can be formed.

The stabilization toward agglomeration can be achieved by electrostatic, steric or electrosteric effects.

Electrostatic stabilization is based on the mutual repulsion of electrical charges. When two similar particles are close to each other, van der Waals forces, resulting from an electromagnetic effect, are always attractive. The addition of a protective agent, such as citrate or tetrakis(hydroxymethyl)-phosphonium chloride (THPC), to the metal precursor (*i.e.* metal halide) generates an electrical double layer of cations and anions. The adsorbed layers result in coulombic repulsions between the particles resulting in the stabilization of the colloid. For example, Baiker and co-workers reported the synthesis of a AuPd catalyst by co-reduction of Au and Pd halides in the presence of tetrahydroxymethylphosphonium chloride (THPC).[22] THPC is an electrostatic stabilizer, the negatively charged Au and Pd precursors coordinate with the positive part of the THPC molecules. During the formation of the metallic sol, a huge excess of NaOH is present. THPC/NaOH acts as the reducing agent *via* formation of formaldehyde, a well-known reducing agent for gold under basic conditions, following the mechanism:[23]

$$P(CH_2OH)_4^+ + OH^- \rightarrow P(CH_2OH)_3 + CH_2O + H_2O$$

Sodium citrate has also been widely used as an electrostatic protective agent in particular for monometallic Au. Sodium citrate acts as a stabilizer as well as a reducing agent. In particular during the metal reduction, it becomes oxidized to the intermediate ketone (acetone dicarboxylic acid), which in return is an even better reducing agent. Guczi's and co-workers used this methodology for the synthesis of a AuPd bimetallic system supported on TiO_2. AuPd nanoparticles were generated in presence of tannin and citrate, in aqueous solution at 338 K and immobilized on TiO_2.[24] The steric

effect was investigated by adsorption of polymers of a sufficiently high molecular weight, forming a protective layer and keeping the nanoparticles at a distance too large to show van der Waals interactions, and, therefore, avoiding agglomeration. Among them, polyvinyl pyrrolidone (PVP) is the most used.

Venezia *et al.* prepared AuPd catalysts on silica using PVP as the protective agent.[25] Au and Pd halide precursors were simultaneously added to a water–ethanol solution containing PVP (metal/PVP ratio = 1 : 5, wt/wt). Silica was added and left under stirring at 363 K for 5 h under N_2 till complete reduction.

Electrosteric stabilization was achieved by the adsorbed polymers having non-negligible electrostatic charges on the metal precursors, resulting in a significant double-layer repulsion. Polyvinyl alcohol (PVA) is a typical example and by far the most employed stabilizer for the generation of AuPd nanoparticles.[26] The effect of the addition sequence of the Au and Pd precursors has been investigated. Au and Pd were reduced in the presence of PVA either simultaneously or by sequential reduction usually using $NaBH_4$ as the reducing agent.

The simultaneous reduction of Au salts in a proper solvent in the presence of a protective agent, followed by their immobilization on a support, has been widely reported.[27] The fundamental step for obtaining bimetallic nanoparticles is the control of the reduction and the nucleation processes of the two metals, because of their different redox potentials and the different chemical nature. Therefore, in order to avoid any segregation of the two metals a proper reducing agent and/or reaction system should be selected.

Prati *et al.* were among the first to prepare PVA-protected AuPd nanoparticles in a liquid phase reaction. Firstly, they reported the formation of an alloy for the preparation of a carbon-supported AuPd (Au : Pd = 1 : 1, molar ratio) bimetallic catalyst using polyvinyl alcohol (PVA) as the protective agent and $NaBH_4$ as the reducing agent, though partial segregated palladium was detected.[27b] On the contrary, Hutchings' group, using the same methodology for preparing AuPd catalysts supported on activated carbon and titania, obtained pure alloys.[27h] This difference could be addressed to the different amounts of polyvinyl alcohol (PVA) used: a PVA/metal ratio of 2 : 1 in the first case and of 1 : 2 in the second. A higher amount of protective agent probably limits the diffusion of Pd on the gold nanoparticles and segregation of Pd is observed.

The second approach utilizes preformed nanoparticles of the first metal, subsequently directing the deposition of the second metal onto the surface with a specific geometry. This method is commonly used to prepare core–shell patterns.[28] When the second metal deposits on the surface of the preformed seeds, a core–shell structure can be obtained, whereas alloy or heterostructures can be synthesized when the deposition and growth of the second metal occurs on a specific site.[27b,29] Moreover, the growth kinetics of the second metal deposition on the preformed seeds can tune the final structure. Different structures have been obtained, for example, for AuPd catalysts, depending on the protective and reducing agent used. The reduction of palladium followed by the one of gold lead to a mixture of the two metals in the colloid solution, due to the weakness of the reducing agent, and only after aging an alloy has been obtained. On the contrary, when Au was deposited on Pd, bimetallic particles were immediately formed without detection of a Pd core and a Au shell. Probably during the addition of Au, the Pd(0) atoms on the nanoparticles are oxidized to Pd^+ with the reduction of Au(III) to Au(0). After the addition of the reducing agent, the Pd ions formed are then reduced again with the formation of a complex structure.

Our group reported the synthesis of a AuPd catalyst by successive reduction of Au in presence of Pd metal sol and of Pd on Au sol before immobilization on carbon.[27b] The reduction was performed using $NaBH_4$ for both metals in the presence of PVA as the protective agent. The bimetallic nanoparticles obtained, with an average diameter of 3.5 nm, showed an alloy structure and the presence of segregated Pd. A second strategy consists of the immobilisation of a preformed gold sol using $NaBH_4$ as reducing agent on activated carbon, and then the sol of palladium was generated in the presence of Au/C using H_2 as a second reducing agent instead of $NaBH_4$.[29] By using H_2 instead of $NaBH_4$ it was possible to slow down the reduction rate of the Pd ions, thus increasing the time of the diffusion and the growth of Pd on Au avoiding any Pd segregation (Fig. 2).

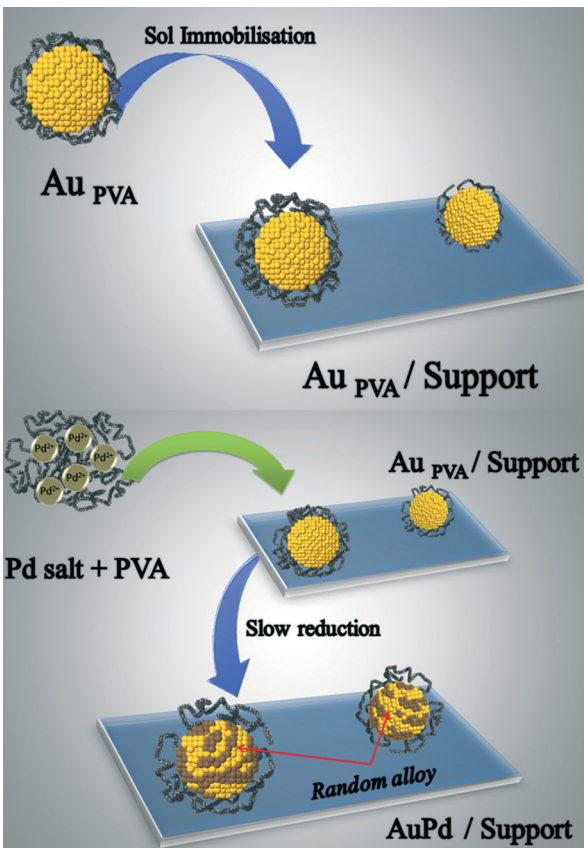

Fig. 2 Two-step procedure for the preparation of a supported uniform AuPd alloy.

The AuPd alloy nanoparticles showed a uniform composition and homogeneity. In further studies, AuPd alloys with different ratios (Au : Pd; 9.5 : 0.5, 9 : 1, 8 : 2, 6 : 4, 2 : 8) have been prepared, using the same procedure, to investigate the effect of the Au/Pd ratio on the final structure of the bimetallic alloy.[30]

Moreover, the role of the protective agent for the Au precursor on the formation of an alloy of uniform composition has been investigated.[31] For this purpose, three different gold precursors have been prepared using a steric stabilizer (PVA) and an electrostatic stabilizer (THPC) or no protective agent (Au prepared using magnetron sputtering). A uniform AuPd alloy could only be obtained when the AuPVA system was used.

With unprotected Au or weakly stabilized Au (THPC), the NPs underwent reconstruction during the deposition/reduction of Pd, not providing efficient seeds for alloying the Pd. In these latter cases, the growing of Au, segregation of the two metals or the formation of different alloy compositions have been observed.

Recently, Tiruvalam *et al.* showed the formation of Pd-core–Au-shell and Au-shell–Pd-core type structures by successive reduction, using a similar methodology to that used in ref. 27*b*.[28] However, as it will be stated in the following section, it is always difficult to prove the presence of a real core–shell structure or Pd-rich or Au-rich bimetallic catalysts for particle sizes below 10 nm.

The impregnation method consists of the direct impregnation of an aqueous solution, containing the metal precursors, with the support in the absence of any protective agent, followed by evaporation of the water. The dried material is further subject to reduction normally using high temperature treatment or gas phase reduction under a H_2 flow.[32] The characteristics of the catalyst strictly depend on the post-treatment conditions (rate of heating, time, final temperature, atmosphere) and, obviously, on the type of supporting material. In fact, during the calcination step, sintering of the precursor and a reaction between the metal precursor and the support might occur. Moreover, the use of different conditions can lead to different metal–support interactions, which is of fundamental importance for catalytic applications. As the effect of temperature is normally detrimental for the metal dispersion, sometimes a reduction step with H_2 or, under basic conditions, with HCHO or $NaBH_4$ has been used instead of calcination.[32] Even though impregnation was shown to produce less active gold catalysts than sol immobilization, the simplicity of the methodology makes impregnation still attractive for industrial scale-up purposes, and because of that, much research has been dedicated to improving this preparation method.[32]

This technique has widely been used for the preparation of AuPd on titania and carbon in particular by Hutchings' group.[33] In a typical preparation, $AuCl_4^-$ is dissolved in water and then $PdCl_2$ is dissolved in the resulting acidic solution. The support is then exposed to the solution, dried (383 K, 16 h) and calcined (673 K, 3 h). Heat treatment steps are very important and control the final morphology obtained. The support plays a fundamental role in the final structure of AuPd. Indeed, on carbon supports random AuPd alloys are formed, whereas for oxidic supports, such as TiO_2, core–shell structures are formed with a gold-rich core and a palladium-rich shell.[11*b*] The heat treatment steps normally lead to bigger particles, which is more evident for carbonaceous supports compared to metal oxides.

Summarizing this part, the advantage of using sol immobilization principally lies within its applicability, regardless of the type of support employed, and the possible control of particle size/distribution, obtaining normally highly dispersed metal catalysts. On the contrary, direct impregnation is drastically affected by the surface properties of the support. It has to be noted that, in the preparation of bimetallic catalysts, particular attention has to be paid to the composition of the single metallic particles in terms of metal ratio and morphology.

Characterization of AuPd

The formation of gold alloys with one additional or even more metals, has greatly increased the possibilities to tailor the structure and therefore the reactivity of the catalysts. The structure complexity increases at the same time. In addition to particle size and shape, the composition, distribution and surface ordering should be taken into consideration for affecting the activity, selectivity and stability of the catalysts. In order to correlate specific sites on the bimetallic systems to catalytic properties, the catalysts' structures need to be characterized at nanometric down to even atomic scale. Complementary X-ray spectroscopic and electron microscopic characterization methods can be used to derive structural information about the atomic configuration on particle surfaces, inside particles and at interfaces.

X-ray techniques determine mainly the average structure of a catalyst. X-ray diffraction (XRD) is widely used to determine the phases present in a catalyst, mainly of the crystalline support and the metallic particles. When metal components with different lattice parameters are segregated, XRD can usually distinguish two different phases. When a random alloy is formed, it can often be detected by precise determination of the changed lattice parameters, which are different from either monometallic counterpart. In addition, according to Vegard's Law[34] and the Rietveld analysis,[35] the ratio of the two alloying metals can be estimated. XRD is also widely used to evaluate the particle size from the width of the diffraction peak.[36] However, it is not sensitive to particles as small as 1–2 nanometers. Therefore, (S)TEM imaging is more preferred for the quantitative measurement of the particle size in the catalyst. Based on high angle annular dark field (HAADF) STEM, several analytical methods have been developed to precisely measure particle size, *e.g.*, by integrating the intensity of the area of cluster to quantify the number of atoms in it, or using a blurring propagation method.[37,38]

X-ray photoelectron spectroscopy (XPS) is a surface sensitive technique, which provides not only the composition on

the particle surface but also the valence states according to the binding energy of the inner shell electrons.[39] It is of particular interest for bimetallic particles, synthesized following different procedures, to control the distribution of the two metals from core–shell structures to random alloys. Some calcined supported AuPd catalysts have been characterized using XPS and showed a Pd-enriched surface, whereby Au was suggested to promote the Pd deposition by electronic effects.[11b,40] Pd^{2+} has been detected using XPS on monometallic Pd catalysts, while, by adding small amounts of Au to form Au : Pd = 1 : 9 bimetallic particles, it is already enough to keep all the Pd atoms as Pd(0). In many publications, it has been reported that the Au $4f_{7/2}$ peak shifts to lower energies by alloying with Pd and shifts even further with decreasing Au concentration.[22,41–43] This could be due to an increased Au 5d occupancy. It was suggested that negatively charged Au could facilitate the extraction of beta hydrogen from alkoxide intermediates.[11] One should also be aware that the material within the depth of a few nanometers may contribute to the photoelectron signals. Therefore, for nanoparticles, the results are weighted toward the top surface atomic layers, but the particle core contributes also attenuated signals.

With X-ray absorption spectroscopy (XAS),[44] the near edge structure of the ionization edges of Au and other metals can be recorded to study the electronic state modification due to alloying as well as due to metal–support interactions. Furthermore, X-ray absorption fine structure (EXAFS) analysis provides unique structural information about the coordination number of a certain type of inter-atomic bonding and about the distances between atoms. Though XAS is not a location specific technique, in combination with TEM and spatially resolved spectroscopy, which reveal the particle size distribution and the composition in nanoparticles, it can provide valuable information about the atomic configuration of the bimetallic nanoparticles. AuPd bimetallic catalysts, following the redox procedure, the colloidal method and other synthetic methods, were characterized using X-ray absorption near edge structure (XANES) and EXAFS.[22,41,42,45] For Au deposited onto activated carbon-supported Pd, XANES analysis of the Pd K edge and Au L edge confirmed that AuPd is in the metallic state, in contrast to oxidative Pd in the monometallic catalyst. EXAFS analysis has shown that the first shell Pd–Pd coordination number does not change much for the bimetallic catalysts compared to the monometallic one. There was a small amount of Pd–Au coordination arising from Au–Pd interactions. These results indicate that Pd particles were relatively unaltered by depositing Au onto them and Au was dispersed on the Pd surface. In contrast, EXAFS characterization of AuPd(sol) catalysts shows more highly dispersed Pd.[45] Therefore, the distribution of Au and Pd is highly dependent on the catalyst preparation method. The coordination numbers of Au–Au, Au–Pd and Pd–Pd were systematically studied for bimetallic catalysts with different Au : Pd ratios[22,41] and different core–shell structures were formed depending on the synthesis method and the Au : Pd ratio. The intensity of the XANES edges often reflects the occupancy of empty orbitals, into which the atomic electrons are excited. For example, it has been reported that the intensity of the Au L_{III} white lines decreased with decreasing particle size, as well as with decreasing Au concentration for AuPd bimetallic catalyst, which was attributed to a higher electron occupancy in Au 5d. The results clearly indicate that highly dispersed Au cluster cause a change in the electronic properties.[22,41,42]

Complementary to the X-ray characterization techniques, TEM provides direct imaging of the catalysts up to atomic resolution and the distribution of the elements can be resolved within individual nanoparticles. High-resolution transmission electron microscopy (HRTEM) and HAADF STEM images can reveal the atomic configuration of small particles with a state-of-the-art spherical aberration corrector[46] for objective and/or probe forming lenses. Therefore, the morphology, crystal structure, surface modification and capping, and straining, due to twinning or metal–support interactions, can be unraveled. Particularly for HAADF STEM, the intensity can be directly correlated to the atomic number and sample thickness along the beam direction forming a so-called "Z-contrast" image, due to its contrast mainly coming from incoherent thermally scattered electrons at high angles.[47] It offers an intuitive interpretation for the HAADF STEM image of supported metal catalysts, where the support usually consists of light atoms, such as C and metal oxide supports. High resolution HAADF STEM images even resolve the position of different metal atoms on a single particle. HAADF STEM is a powerful application used to study AuPd bimetallic structures (Fig. 1), as shown in Fig. 3. More practically, energy dispersive X-ray spectra can be acquired in STEM

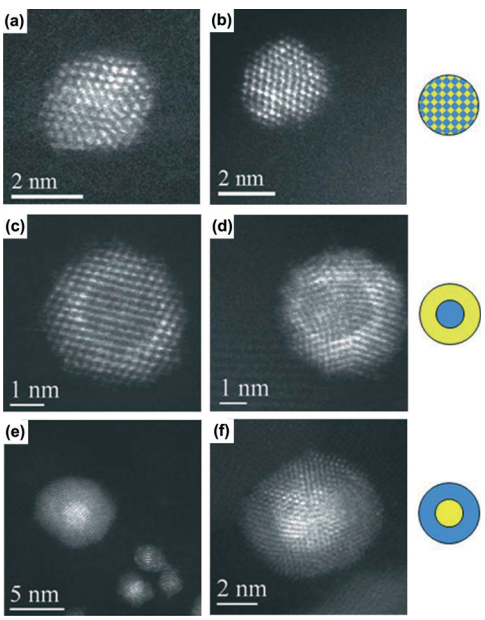

Fig. 3 Representative HAADF-STEM images of individual sol-immobilized (Au + Pd) (a), Au{Pd} (c), Pd{Au} (e) NPs on activated carbon; and (Au + Pd) (b), Au{Pd} (d), Pd{Au} (f) NPs on TiO_2 after drying at 120 °C for 16 h. Reproduced from ref. 28 with permission from The Royal Society of Chemistry.

mode with a focused electron beam in the sub-nanometer range. Recently, combining probe-corrected STEM with an in column silicon drift detector has improved the resolution and the detector efficiency greatly, so that core–shell structures, segregations and random alloys within individual particles can be unambiguously distinguished.

Efforts have been dedicated to the synthesis of different types of bimetallic nanoparticles and to their characterization using advanced TEM techniques.[48–53] It has been unraveled that the structure of a bimetallic catalyst is dependent on the support material, the synthesis procedure and the post-treatment of the as-prepared catalysts. The inhomogeneity in the composition and distribution is usually related to the ratio of the alloyed metals and the specific particle size. For example, for catalysts prepared by co-impregnation of the support using the incipient wetness with aqueous solutions of $PdCl_2$ and $HAuCl_4$, followed by calcination at 400 °C, the AuPd particles on TiO_2 and Al_2O_3 as supports were found to exhibit a core–shell structure, Pd being concentrated on the surface. In contrast, the AuPd/carbon catalyst exhibited AuPd nanoparticles which were homogeneous alloys. The structures of bimetallic catalysts synthesized using the sol immobilization method can be controlled by the reduction sequence of the metal precursors, namely $PdCl_2$ and $HAuCl_4$. Random alloy, Au-core–Pd-shell and Pd-core–Au-shell structures can be formed by the reduction of mixed precursor solutions, of $PdCl_2$ in the presence of Au(0) and of $HAuCl_4$ in the presence of Pd(0), respectively.[28] A STEM-EDX spectrum image analysis is presented in Fig. 4, where both reconstructed RGB maps of Au and Pd, and integrated EDX spectra from the center and the periphery of the particle, confirmed a Pd-core–Au-shell structure. A similar successive reduction method has been used to produce three-layer core–shell particles, which consist of an alloyed inner core, a Au-rich intermediate layer, and a Pd-rich outer shell, as revealed by HAADF STEM and EDX analysis.[54] The order of metal addition and reduction during the initial sol formation affects not only the activity, but also the selectivity. A series of catalysts with varying Au : Pd ratios (9.5 : 0.5 to 2 : 8) were synthesized following a two-step procedure.

Using HRTEM and STEM-EDX mapping, it has been suggested that good alloy particles can be formed from the Au : Pd ratios of 9 : 1, 8 : 2, and 6 : 4, while the catalysts with Au : Pd = 9.5 : 0.5 and Au : Pd = 2 : 8 consist of segregated Pd particles and were considered as the reason for low activity and quick deactivation in the oxidation of glycerol.[30b]

In the liquid phase oxidation of benzyl alcohol, it was found that the structure of the catalyst particles changes dynamically with the reaction proceeding.[55] Physically mixed Au/AC and Pd/AC (AC = activated carbon) were used as starting catalysts. The *in situ* formation of surface Au–Pd bimetallic sites, by the reprecipitation of Pd onto Au nanoparticles, was verified using STEM-EDX mapping of the catalysts after 0.5 h and 1 h of reaction. Fig. 5 shows the STEM image, the Au and Pd maps and the overlap of the two maps of a few alloy particles formed after one hour of reaction. The Pd concentration increased with time on the initial Au particles. Negligible Au leaching was observed. When the bimetallic sites were formed Au stabilized the Pd atoms, thereby preventing Pd aggregation and leaching, which leads to the deactivation of the catalyst. Until now not much has been done investigating of the dynamical structure change during the liquid phase reaction, which is partially due to difficulties in applying *in situ* characterization techniques to liquid systems. Nonetheless, depending on the miscibility of the alloying metals, the detailed structure of the bimetallic particles and the reaction conditions, one would expect that the catalysts commonly undergo changes during reactions,

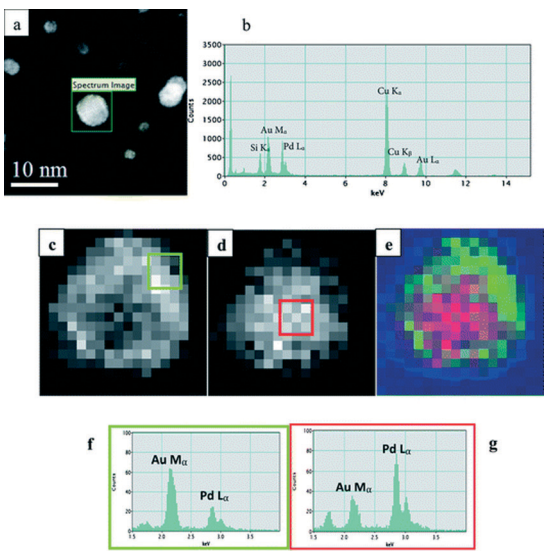

Fig. 4 (a) An ADF image of a Au{Pd} nanoparticle selected for STEM-XEDS mapping; (b) the overall XEDS spectrum of the nanoparticle showing the presence of both Au and Pd. (c, d) The Au and Pd elemental maps of the nanoparticle obtained after MSA processing. (e) An RGB reconstruction showing the distribution of Au (green) and Pd (red) —the blue channel is neutral. (f, g) The cumulative XEDS spectra of areas (3 × 3 pixels) (indicated by squares in (c & d)) from the center and the periphery of the particle, respectively. Reproduced from ref. 28 with permission from The Royal Society of Chemistry.

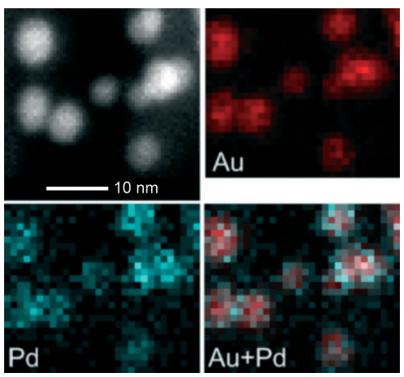

Fig. 5 STEM images, Au and Pd maps and overlap of the two maps showing a part of the original physically mixed Au/AC catalyst after 1 hour of reaction in benzyl alcohol oxidation. Reproduced with permission from ref. 30*b*. Copyright© 2010 WILEY-VCH.

leading to segregation or enhanced alloying, which greatly influence the ultimate activity, selectivity and stability of the catalyst.

As we can see from the above discussion, X-ray and TEM characterizations can provide complementary structural information for the determination of geometric and electronic structures of bimetallic nanoparticles. By different synthetic procedures, the structures of the nanocatalysts can be tailored to some extent and therefore their activity and selectivity can be controlled.

Catalytic applications

Benzyl alcohol oxidation

Benzyl alcohol oxidation has been extensively used as a model reaction in particular for aromatic activated alcohols.[6] Depending on the reaction conditions (temperature, solvent, oxygen pressure), many side-products including benzene, benzoic acid, benzyl benzoate, and toluene have been reported to be formed beside the main product, benzaldehyde, as shown in Scheme 1.

Many papers reporting the utilization of AuPd systems in benzyl alcohol oxidation are present in the literature, but an exhaustive comparison is not possible due to the different reaction conditions used. Typically, these reactions are performed in a batch reactor under mild conditions in the temperature range 333–393 K and with a partial pressure of O_2 of 1–10 bar, in the presence of solvents, such as cyclohexane, toluene and water, or under solventless conditions.

Different preparation methods, in particular sol immobilization, with PVA as the protective agent, and impregnation have been used. Moreover, a wide range of supports, such as activated carbon, carbon nanotubes, TiO_2, SiO_2 and polymers have been considered.[6,9] Some examples are reported in Table 1.

Prati's group was among the first to demonstrate the efficiency of the sol immobilization method for making uniform pure AuPd alloys supported on activated carbon and to test this catalyst for alcohol oxidation in the presence of O_2.[11a] It was demonstrated that the existence of the AuPd alloy

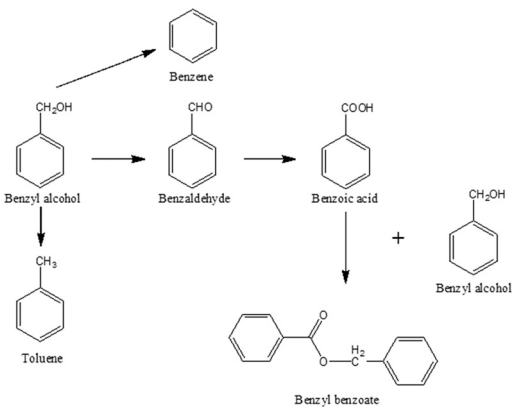

Scheme 1 Reaction scheme for benzyl alcohol oxidation.

increases the catalytic activity compared to monometallic Pd (TOF of 38 to 54 h^{-1} for Pd and AuPd, respectively) (entries 1 and 2, Table 1), keeping a very high selectivity (>94%) toward benzaldehyde. Note that under the same conditions Au was inactive. The better activity has been ascribed to a geometric effect. Indeed, in AuPd the interatomic distances are different to those in the pure metals.[29] A significant improvement in the catalytic activity was found when water was used as solvent instead of toluene, with the TOF value increasing from 54 h^{-1} in toluene to 985 h^{-1} in water (entry 5, Table 1). The beneficial effect of water could be ascribed to the modified affinities of the substrates for the hydrophobic catalyst surface of the activated carbon, favoring the adsorption of the alcohol and the desorption of the carbonyl compound. Moreover, the abstraction of the hydride, the rate-determining step in the oxidative dehydrogenation of the alcohol, is favored in the presence of water, which acts as a weak base.[6] Interestingly, under these reaction conditions, the presence of water as solvent did not show any effect on the selectivity with benzaldehyde as the unique product. The AuPd alloy did not only show a higher activity than Pd but also a better resistance to deactivation.[27g,56] The presence of Au, indeed, drastically limits the deactivation, which is typical of Pd, due to leaching of the metal and deactivation by O_2 poisoning.[11a] Using the same preparation method, the general applicability of the single phase alloy was demonstrated with the Au/Pd molar ratio varying from 9 : 1 to 2 : 8 (entries 3–10, Table 1). The best performance was obtained when uniform alloyed bimetallic nanoparticles were obtained (Au/Pd ratios 9 : 1–6 : 4, entries 3–5, Table 1), and in particular Au8–Pd2/AC was the most efficient catalyst (entry 4, Table 1). On the contrary, in Au2–Pd8/AC, Pd monomer sites, isolated by Au atoms, were present, showing a slightly lower activity (entry 6, Table 1). Moreover, it has been shown that, as expected, the addition of a base increases the activity of the catalysts (entries 7–10, Table 1). It is well known that the presence of a base favors the abstraction of the hydride, the limiting step for Au-catalyzed alcohol oxidation.[6] Interestingly, this effect is more evident for catalysts with a Au-rich composition. The authors stated that in gold-rich compositions the rate determining step is the H-abstraction; whereas in the palladium rich composition it is the H-transfer from Pd–H, where the base has a negligible effect.[57] The addition of a base was detrimental in terms of selectivity with the formation of benzoic acid and benzyl benzoate in high amounts, for all the catalysts (entries 7–10, Table 1). Another interesting study from this group showed that a AuPd alloy was formed *in situ* starting from a physical mixture of Au/AC and Pd/AC in the benzyl alcohol oxidation in water. After 1 h of reaction, the physical mixture showed a similar catalytic activity to the AuPd/AC alloy. TEM characterization, performed on the used catalyst, showed the partial formation of a AuPd alloy, probably due to the migration of the Pd species onto the Au nanoparticles.[58]

Hutchings' group extensively studied the effect of the AuPd morphology, in particular when supported on TiO_2, on

Table 1 Comparative data for benzyl alcohol oxidation

		Reaction conditions					Selectivity				
Entry	Catalyst	Solvent	T (K)	pO_2 (bar)	Metal/sub. ratio	TOF	Benzaldehyde	Toluene	Benzyl benzoate	Benzoic acid	Ref.
1	1% Pd/AC	Toluene	333	1.5	1/500	38	>99	—	—		11
2	1% Pd40@(Au60/AC)	Toluene	333	1.5	1/500	54	94	—	—	—	11
3	1% Pd10@(Au90/AC)	Water	333	1.5	1/500	780	>99	—	—	—	57
4	1% Pd20@(Au80/AC)	Water	333	1.5	1/500	1021	>99	—	—	—	57
5	1% Pd40@(Au60/AC)	Water	333	1.5	1/500	985	>99	—	—	—	57
6	1% Pd80@(Au20/AC)	Water	333	1.5	1/500	716	>99	—	—	—	57
7	1% Pd10@(Au90/AC)[a]	Water	333	1.5	1/500	1140	28	—	32	40	57
8	1% Pd20@(Au80/AC)[a]	Water	333	1.5	1/500	1189	46	—	22	32	57
9	1% Pd40@(Au60/AC)[a]	Water	333	1.5	1/500	1071	45	—	24	31	57
10	1% Pd80@(Au20/AC)[a]	Water	333	1.5	1/500	776	50	—	24	26	57
11	5% Au50–Pd50/TiO_2	None	383	1	Nd	14 270	Nd	Nd	Nd	Nd	11*b*
12	5% Au50–Pd50/TiO_2	None	393	1	Nd	26 400	Nd	Nd	Nd	Nd	11*b*
13	5% Au50–Pd50/TiO_2	None	433	1	Nd	86 500	Nd	Nd	Nd	Nd	11*b*
14	1% Au + Pd/AC_{SI}	None	393	10	1/55 000	1800	79	2	—	4	27*f*
15	1% Au + Pd/AC_I	None	393	10	1/55 000	500	69	10	—	3	27*f*
16	1% Au + Pd/TiO_2	None	393	10	1/55 000	15 360	69	27	2	2	27*g*
17	1% Pd50@Au50/TiO_2	None	393	10	1/55 000	19 250	77	18	3	2	27*g*
18	1% Au50@Pd50/TiO_2	None	393	10	1/55 000	17 360	72	23	3	2	27*g*
19	1% Au50 + Pd50/AC	None	393	10	1/55 000	35 400	55	41	2	1	27*g*
20	1% Pd50@Au50/AC	None	393	10	1/55 000	41 930	63	35	0	2	27*g*
21	1% Au50@Pd50/AC	None	393	10	1/55 000	24 310	65	29	3	3	27*g*
22	1% Au + Pd/TiO_2 calc. 673 K	None	393	10	1/55 000	3940	70	22	6	2	27*g*
23	1% Pd50@Au50/TiO_2 calc. 673 K	None	393	10	1/55 000	8650	72	21	5	2	27*g*
24	1% Au50@Pd50/TiO_2 calc. 673 K	None	393	10	1/55 000	8780	69	25	4	1	27*g*
25	1% Au50 + Pd50/AC calc. 673 K	None	393	10	1/55 000	2490	79	2	10	4	27*g*
26	1% Pd50@Au50/AC calc. 673 K	None	393	10	1/55 000	2430	75	3	13	4	27*g*
27	1% Au50@Pd50/AC calc. 673 K	None	393	10	1/55 000	3410	79	5	11	4	27*g*
28	1% Pd40@(Au60/CNFs)	None	393	1.5	1/35 000	6076	74	18	3	1	64
29	1% Pd40@(Au60/N-CNFs)	None	393	1.5	1/35 000	52 638	76	11	7	5	64
30	2% Au70 + Pd10/PANI[a]	Toluene	373	1	1/150	16	71	Nd	Nd	Nd	21
31	2% Au50 + Pd50/PANI[a]	Toluene	373	1	1/150	16	82	Nd	Nd	Nd	21
32	2% Au10 + Pd90/PANI[a]	Toluene	373	1	1/150	14	98	Nd	Nd	Nd	21
33	3Au–1Pd/APS-S16	None	413	1	Nd	4052	89	11	Nd	0	65
34	1Au–1Pd/APS-S16	None	413	1	Nd	4715	94	6	Nd	0	65
35	1Au–2Pd/APS-S16	None	413	1	Nd	6575	94	5	Nd	1	65
36	1Au–3Pd/APS-S16	None	413	1	Nd	7864	91	8	Nd	1	65
37	1Au–5Pd/APS-S16	None	413	1	Nd	8667	94	5	Nd	1	65
38	1% Au–0.5% Pd/γ-Al_2O_3	Toluene	333	1	1/500	5.5	81	—	19	—	63
39	1% Au + 0.5% Pd/γ-Al_2O_3	Toluene	333	1	1/500	26.4	84	—	14	—	63
40	1% Pd40@(Au60/AC)	Cyclohexane	353	2	1/5000	2261	89	8	2	1	68
41	0.1% Bi + 1% Pd40@(Au60/AC)	Cyclohexane	353	2	1/5000	2546	95	2	3	0	68
42	3% Bi + 1% Pd40@(Au60/AC)	Cyclohexane	353	2	1/5000	1643	97	1	2	0	68
43	1% Au50 + Pd50/TiO_2	None	393	10	1/10 0000	63 800	67	3	7	23	69
44	1% Au45 + Pd45 + Pt10/TiO_2	None	393	10	1/10 0000	31 900	80	—	6	13	69

[a] Addition of NaOH.

alcohol oxidation. They showed that AuPd alloys, prepared using the impregnation method, are particularly efficient for the solvent-free benzyl alcohol oxidation in the presence of molecular oxygen.[11b] Under these reaction conditions, very high activities were detected, with the TOF value increasing from 14 270 h^{-1} to 86 500 h^{-1}, when increasing the reaction temperature from 383 K to 433 K (entries 11–13, Table 1). The high activity was attributed to the formation of a Au-rich core/Pd-shell structure, with an electron promotion effect for Au on Pd.[11b] Also for these systems, the effect of the Au : Pd ratio has been investigated and it was determined that AuPd with a 1 : 1 weight ratio produced the highest catalytic activity.[11b] Interestingly it was reported that the Au/Pd ratio has an important effect also on the selectivity. Indeed, with Pd-rich compositions a selectivity of 66–70% toward benzaldehyde was observed with the production of 21% toluene, whereas Au-rich compositions yielded up to 95% of benzaldehyde, suppressing the formation of toluene. In following studies, the same group compared the catalytic activity of AuPd catalysts supported on activated carbon either prepared using sol immobilization (entry 14, Table 1) or impregnation (entry 15, Table 1). In both cases, a homogenous alloy was obtained. The higher catalytic performance of AuPd prepared by sol immobilization was attributed to the different particle

size and the size distribution. Indeed, it is well accepted that liquid phase oxidation is a size-dependent reaction, where smaller particles are more active than bigger ones.[7] Indeed, for sol immobilization prepared catalysts, AuPd particles of 5 nm have been obtained, whereas for those prepared using impregnation larger AuPd particles of 3–8 nm have been obtained as well as particles up to >20 nm.[59] The effect of random alloys *versus* core–shell structures has also been investigated, preparing AuPd nanoparticles *via* sol immobilization and using titania and activated carbon as supports.[27g,28] For this purpose, AuPd nanoparticles were synthesized using co-reduction of the two metals (Au + Pd) or sequential reduction of Au and Pd (Pd@Au) or *vice versa* Au@Pd. HAADF STEM measurements confirmed that a AuPd alloy was obtained by co-reduction, whereas a core–shell structure was created by sequential addition of the two metals. The catalysts were tested in the benzyl alcohol oxidation under solventless conditions at 393 K (entries 16–27, Table 1). The order of metal addition has a significant effect on the catalytic activity, and the most active catalyst had a Au-core–Pd-shell structure, regardless of the support used (entries 17 and 20, Table 1). On the contrary, the order of metal addition did not appreciably influence the selectivity.

The support has a stronger effect on both the activity and the selectivity than the order of addition: AC supported catalysts showed a better activity (entries 19–21, Table 1), whereas those supported by TiO_2 showed a better selectivity to benzaldehyde with a limited production of toluene (entries 16–18, Table 1).

In these studies, calcination has been performed (673 K in air) in order to remove the PVA from the metal surface and the effect of PVA on the catalytic performance has been investigated.[27g,28] The high temperature used efficiently removed the PVA from the surface, but affected the morphology of the catalyst and the general growth of the AuPd particles, which was more evident in the activated carbon supported catalysts.[28] As a consequence, all the catalysts showed a lower activity than those untreated (entries 23–27, Table 1).

Beyond PVA, other protective agents have been proposed for the generation of AuPd nanoparticles to be used in the oxidation reaction. Baiker's group, for example, reported the synthesis of THPC-protected AuPd nanoparticles, supported on PANI, varying the AuPd ratio from 7 : 1 to 1 : 9 and the utilization in the oxidation of benzyl alcohol, using water as solvent and NaOH.[22] The catalysts yielded full conversions, but they did not show appreciable TOFs (14–16 h^{-1}) compared to the previously reported systems, even in the presence of NaOH (entries 30–32, Table 1). It is also interesting to note that a very high selectivity toward benzaldehyde was achieved (71–98%) compared to previously described Au*X*Pd*Y*/AC (28–50%) (entries 7–10, Table 1). Benzoic acid was not detected and they probably addressed the absence by monitoring the formation of amides, formed from benzoic acid and the amines present on PANI.[22]

Different groups developed different strategies, such as incipient wetness,[60] grafting,[61] and Ar glow-discharge plasma reduction,[62] for introducing the AuPd nanoparticles inside the framework of SBA-15 to increase the stability of the catalytic systems during the reaction. The catalysts showed a good resistance to deactivation during the recycling tests, due to limited leaching of the metal which occurred probably due to a steric confinement inside the mesopores of SBA-15.

Evangelisti *et al.* proposed an alternative procedure to generate supported AuPd nanoparticles using metal vapor synthesis with alumina as the support. They showed that the AuPd alloy system, prepared by direct vaporization of the two metals (entry 39, Table 1), is more active than the physical mixing of separately prepared Au and Pd precursors (entry 38, Table 1), as already pointed out for the wet preparation synthesis.[63]

Recently, it has been shown that the support is an important factor dictating the overall activity of the metal nanoparticles in particular in the liquid phase reaction.[5a,b] Indeed, the support properties can create different interactions with the metallic particles immobilized on the surface or inside the pore structure, thus modifying both their electronic and structural properties. In addition, the support can also provide different anchoring sites for the reactants or play an active role in the catalytic reaction. It is normally recognized that surface's acidic and basic functionalities provide a better dispersion of MNPs which contributes to an increase in catalytic activity. In addition, basic functionalized surfaces can speed up the oxidation rate, favoring the H-abstraction.

Many studies, present in the literature, address the support effect on Au or Pd nanoparticles. However, only few examples are present for bimetallic AuPd.

Villa *et al.* reported the immobilization of PVA-protected AuPd nanoparticles on bare carbon nanofibers (CNFs) and nitrogen-functionalized carbon nanofibers (N-CNFs).[64] The nitrogen groups were introduced to the support framework using gas phase treatment with ammonia at 873 K, increasing the basicity of the support. The improvement in the catalytic performance of the AuPd/N-CNFs in the solvent free benzyl alcohol oxidation was attributed to a better dispersion of the metal nanoparticles on the surface as well as to the increased local basic environment, compared to the AuPd/CNFs (entries 28, 29, Table 1).

A similar strategy was adopted by Chen *et al.*, impregnating Au*X*Pd*Y* onto amino-functionalized SBA-16. All the catalysts, consisting of pure alloys, revealed a good activity in the solventless oxidation of benzyl alcohol, with the Pd-rich composition being the most active (entries 33–37, Table 1). Moreover, the presence of the amino groups increased the durability of the catalysts, maintaining the same catalytic performance during the recycling tests.[65]

AuPd nanoalloys supported on Mg–Al oxides showed a better performance than those supported on CeO_2 and SiO_2, which is, according to the authors, due to the strong dehydrogenation ability of the Mg–Al oxides, facilitating the H-abstraction.[66]

In all the studies reported it has been shown that the main problem that affects the selectivity for benzaldehyde during the benzyl alcohol oxidation, is the parallel production of toluene. Two principal mechanisms were proposed for the toluene formation: the disproportionation of two benzyl alcohol molecules to form equimolar benzaldehyde and toluene or the reaction of the intermediate metal-hydride with the alcohol instead of O_2.[6]

In recent literature, different strategies in order to depress the toluene formation are reported, in particular, the design of new catalysts is described by varying the support or introducing a metal that acts as a modifier of the AuPd active sites. Sankar *et al.* showed that in the case of AuPd/TiO_2 the disproportionation of benzyl alcohol is the main source of toluene.[67] By choosing appropriate supports, such as MgO and ZnO, the disproportionation reaction could be depressed with a consequent increase in benzaldehyde.[67] Prati's group showed that the addition of 0.1% Bi and 3% Bi to AuPd/AC increased the selectivity toward benzaldehyde from 89% for AuPd to 95 and 97% for 0.1% Bi–AuPd and 3% Bi–AuPd, respectively.[68] This effect could be mainly ascribed to the blocking of a fraction of the active sites which are responsible for a different substrate coordination. In this case, the parallel pathway that yields toluene has been suppressed. However, the amount of Bi introduced in AuPd has a different effect on the activity. The addition of 0.1% Bi has a positive effect on the activity of the catalyst (TOF: 2546 h^{-1} and 2261 h^{-1} for 0.1% Bi–AuPd and AuPd, respectively) (entries 40–41, Table 1). On the contrary, higher Bi loading (3%) has a detrimental effect (TOF: 1643 h^{-1}) (entry 42, Table 1). The promoting effect of Bi can be attributed to an electronic effect. However, when Bi is present in higher amounts it can block some of the AuPd active sites.

Similarly, He *et al.* showed that the addition of Pt to AuPd/TiO_2, with the formation of a random ternary alloy, decreases the activity but increases the selectivity toward benzaldehyde from 67% to 80%, suppressing the formation of toluene and limiting the formation of benzoic acid (entries 43, 44, Table 1).[69]

CO oxidation

The catalytic oxidation of CO has been extensively studied, in particular using monometallic catalysts. On the contrary, only few examples on the use of Au bimetallic catalysts, in particular AuPd, are present.[15a] The reaction can be described using the equation: $CO + 0.5O_2 \rightarrow CO_2$, and can be considered the pivotal reaction which mostly contributes to the success of gold in catalysis.

The first attempt of using AuPd bimetallic catalysts involved the use of catalysts prepared by sol immobilization of protected AuPd nanoparticles. It should be highlighted, however, that the protective agent has to be removed from the metal surface, for example, by heat treatment, in order to obtain active catalysts for the gas phase CO oxidation. Conversely, this post-treatment is not required for the liquid phase oxidation, where the protective agent only partially decreases the catalytic performance. The reason for the different trend is still not clear. Probably, in the liquid phase, the solvent is able to remove the protective agent from the active sites during the reaction. In addition, the protective layer branches can have a different geometrical structure in the two phases, making the active sites accessible to the reactant only in the liquid phase.

Guczi's group was the first to report the synthesis of a AuPd bimetallic system for this reaction. AuPd nanoparticles were generated in the presence of tannin and citrate, which act as the protective and reducing agents, and then deposited on TiO_2.[24] The samples were calcined at 400 °C for 1 h in an O_2/He mixture, in order to remove the protective agents from the metal surface, and then reduced in H_2 at 200 °C. This treatment was efficient in the removal of the organic layer but yielded a particle growth from 4.3 to 9.6 nm. XAS characterization evidenced the presence of the AuPd alloy, though segregated Pd was not excluded. Surprisingly, CO oxidation, performed at 60 °C with a mixture of 5.6 mbar CO and 91.8 mbar O_2 in He, showed that the activity of the AuPd bimetallic system is only slightly higher than the activity of a Au + Pd physical mixture, evidencing only a minimal synergistic effect. In a successive study, the authors compared different AuPd/TiO_2 systems, prepared using the same methodology, by investigating the effect of co-reduction or sequential reduction of the two metals.[70] An alloy structure has been found in all the cases and XPS revealed a Pd enrichment in the case of Pd deposited on Au. The three different bimetallic systems obtained showed, however, a similar activity. Therefore, the activity seems not to be significantly influenced by the surface composition of the bimetallic system. Moreover, it has been observed that, as shown in a previous report, the AuPd alloy is almost as active as the Au + Pd physical mixture.

The same group reported the synthesis of AuPd nanoparticles supported on silica, prepared using sol immobilization with PVP as the stabilizer.[25] The stabilizer has been removed *via* calcination at 673 K before testing the catalyst in CO oxidation at 413 K. The effect of the Au/Pd ratio has been studied and it has been varied from 1 : 9 to 9 : 1 (molar ratio). XRD measurements evidenced the presence of AuPd alloys with mean particle sizes of 12–24 nm after calcination. All catalysts showed a low activity compared to data present in the literature, probably due to the large size of the AuPd nanoparticles. In these two cases, the limited synergistic effect is due to the absence of a homogenous alloy and the presence of both alloyed and segregated metals.

Scott *et al.* reported the synthesis of AuPd catalysts prepared using amino-terminated poly(amidoamine) dendrimer-encapsulated nanoparticles with $NaBH_4$ as the reducing agent.[71] The AuPd nanoparticles were supported on TiO_2, and calcined at 773 K in O_2, to remove the organic layer from the metal surface, and then treated in a H_2 flow. The AuPd average particles size only slightly increased during the calcination step, from 1.8 to 3.2 nm. EDS analyses of individual

nanoparticles confirmed the presence of a AuPd alloy with almost the same atomic composition. Interestingly, in this case a strong synergistic effect has been evidenced. Indeed, AuPd starts to be active at 150 °C, whereas monometallic Au and Pd are completely inactive.

El-Shall *et al.* proposed a microwave irradiation method for the preparation of AuPd nanoparticles in a mixture of oleyl amine and oleic acid as the capping and reducing agents, supported on CeO_2.[72] The presence of a AuPd alloy was proven in XRD and TEM measurements. The AuPd alloy showed a higher activity compared to monometallic Pd only at low temperatures (<333 K).

TiO_2-supported AuPd with a Au/Pd atomic ratio of 8 was prepared using deposition–precipitation with urea, followed by reduction under H_2 at 773 K.[73] XPS and diffuse reflectance infrared Fourier transform spectroscopy (DRIFTs) analysis evidenced the presence of a AuPd alloy with partial segregation of Au. Interestingly, the AuPd surface composition was monitored using environmental high resolution electron microscopy (ETEM) and (DRIFTs) during the exposure to O_2 and CO/O_2, evidencing Pd segregation at the surface with the formation of a Au-core–Pd-shell structure. The AuPd alloy showed a better activity in the low temperature CO oxidation than monometallic Au. However, the authors observed a higher rate of deactivation in $AuPd/TiO_2$ compared to Au/TiO_2, probably due to the replacement of Au in the low coordination sites which are considered the most active sites in CO oxidation, by Pd atoms.[74]

Goodman and co-workers investigated CO oxidation on planar AuPd surfaces deposited on Mo(110) as well as on TiO_2-supported AuPd nanoparticles to understand the synergistic effect of the AuPd alloy compared to monometallic Pd and Au using Polarization-Modulation Infrared Reflection Absorption Spectroscopy (PM-IRAS) and kinetic studies.[75] At a low pressure (1.3×10^{-7} mbar), Pd resulted in a higher activity than the corresponding AuPd alloy. Indeed, when alloying Au with Pd, isolated Pd sites are formed which are not able to dissociate O_2.[76] It should be noted indeed, that chemisorbed O_2 must react as dissociated oxygen in order to form CO_2. At a higher pressure (20 mbar), at which the studies cited above are normally performed, Pd preferentially segregated at the surface, as evidenced by Delannoy *et al.*, forming contiguous Pd sites which are able to dissociate O_2.[73]

Moreover, Pd is deactivated faster than AuPd, due to the stronger CO binding and the higher tendency to be passivated by oxygen compared to the alloy surface.

Concluding remarks

Gold has been studied for a long time as a potential alternative to Pd or Pt catalysts. Indeed, its catalytic activity has been shown to be often advantageous especially in terms of selectivity and durability. Therefore, a lot of efforts have been done to combine the peculiar properties of gold with the already well-established ones of other catalytically active metals.

Focussing on Pd-based catalysts, this paper reviewed the main results obtained due to the addition of Au using two specific applications, namely the oxidation of benzylic alcohol in the liquid phase and CO oxidation in the gas phase. It clearly appears that modifying Pd catalysts with Au can have different effects, depending on the nature of the bimetallic species, though generally a positive effect has been claimed.

Particular attention should be paid to the real nature of the obtained bimetallic species, as it strongly affects the catalytic activity and selectivity. Therefore, the characterization of the representative species plays a crucial role in investigating the catalytic properties. Moreover, it has been shown that this task is not trivial and should be carefully executed to be really representative of the whole catalytic material.

Notes and references

1 (*a*) M. A. El-Sayed, *Acc. Chem. Res.*, 2001, **34**, 257; (*b*) K. G. Thomas and A. V. Kamat, *Acc. Chem. Res.*, 2003, **36**, 888; (*c*) M. C. Daniel and D. Astruc, *Chem. Rev.*, 2004, **104**, 293; (*d*) E. C. Dreaden, A. M. Alkilany, X. Huang, C. J. Murphy and M. A. El-Sayed, *Chem. Soc. Rev.*, 2012, **41**, 2740; (*e*) Y. Zhang, X. Cui, F. Shi and Y. Deng, *Chem. Rev.*, 2012, **112**, 2467.
2 M. Haruta, T. Kobayashi, H. Sano and N. Yamada, *Chem. Lett.*, 1987, 405.
3 G. J. Hutchings, *J. Catal.*, 1985, **96**, 292.
4 (*a*) G. C. Bond and D. T. Thompson, *Catal. Rev.: Sci. Eng.*, 1999, **41**, 319; (*b*) G. C. Bond, C. Louis and D. T. Thompson, *Catalytic Science Series*, ed. G. J. Hutchings, ICP Covent Garden, London, 2006, vol. 6.
5 (*a*) M. Haruta, *Catal. Today*, 1997, **36**(1), 153; (*b*) L. Prati, A. Villa, A. R. Lupini and G. M. Veith, *Phys. Chem. Chem. Phys.*, 2012, **14**, 2969; (*c*) A. Villa, M. Schiavoni and L. Prati, *Catal. Sci. Technol.*, 2012, **2**, 673; (*d*) X. Y. Liu, A. Wang, T. Zhang and C.-Y. Mou, *Nano Today*, 2013, **8**, 403.
6 T. Mallat and A. Baiker, *Chem. Rev.*, 2004, **104**, 3037.
7 (*a*) S. Carrettin, P. McMorn, P. Johnston, K. Griffin, C. J. Kiely and G. J. Hutchings, *Phys. Chem. Chem. Phys.*, 2003, **5**, 1329; (*b*) F. Porta and L. Prati, *J. Catal.*, 2004, **224**, 397.
8 A. K. Singh and Q. Xu, *ChemCatChem*, 2013, **5**, 652.
9 (*a*) N. Dimitratos, J. A. Lopez-Sanchez and G. J. Hutchings, *Chem. Sci.*, 2012, **3**, 20; (*b*) S. E. Davis, M. S. Ide and R. J. Davis, *Green Chem.*, 2013, **15**, 17.
10 (*a*) C. George, A. Genovese, A. Casu, M. Prato, M. Povia, L. Manna and T. Montanari, *Nano Lett.*, 2013, **13**, 752; (*b*) J. Xu, T. White, P. Li, C. He, J. Yu, W. Yuan and Y.-F. Han, *J. Am. Chem. Soc.*, 2010, **132**, 10398.
11 (*a*) N. Dimitratos, A. Villa, D. Wang, F. Porta, D. Su and L. Prati, *J. Catal.*, 2006, **244**, 113; (*b*) D. I. Enache, J. K. Edwards, P. Landon, B. Solsona-Espriu, A. F. Carley, A. A. Herzing, M. Watanabe, C. J. Kiely, D. W. Knight and G. J. Hutchings, *Science*, 2006, **311**, 362.
12 J. K. Edwards, S. J. Freakley, A. F. Carley, C. J. Kiely and G. J. Hutchings, *Acc. Chem. Res.*, 2014, **47**, 845.

13 L. Kesavan, R. Tiruvalam, M. H. A. Rahim, M. I. bin Saiman, D. I. Enache, R. L. Jenkins, N. Dimitratos, J. A. Lopez-Sanchez, S. H. Taylor, D. W. Knight, C. J. Kiely and G. J. Hutchings, *Science*, 2011, **331**, 195.

14 (*a*) D. Martin Alonso, S. G. Wettsteina and J. A. Dumesic, *Chem. Soc. Rev.*, 2012, **41**, 8075; (*b*) H. Zhanga and N. Toshima, *Catal. Sci. Technol.*, 2013, **3**, 268.

15 (*a*) A. Kumar Singh and Q. Xu, *ChemCatChem*, 2013, **5**, 652; (*b*) A. Wanga, X. Y. Liu, C.-Y. Moub and T. Zhang, *J. Catal.*, 2013, **308**, 258.

16 R. Ferrando, J. Jellinek and R. L. Johnston, *Chem. Rev.*, 2008, **108**, 845.

17 (*a*) M. A. K. Khalil and R. A. Rasmussen, *Science*, 1984, **224**, 54; (*b*) X. W. Xie, Y. Li, Z. Q. Liu, M. Haruta and W. J. Shen, *Nature*, 2009, **458**, 746.

18 (*a*) M. V. Twigg, *Appl. Catal., B*, 2007, **70**, 2; (*b*) R. M. Heck and R. J. Farrauto, *Appl. Catal., A*, 2001, **221**, 443; (*c*) S. Royer and D. Duprez, *ChemCatChem*, 2011, **3**, 24.

19 Q. Fu, W. X. Li, Y. X. Yao, H. Y. Liu, H. Y. Su, D. Ma, X. K. Gu, L. M. Chen, Z. Wang, H. Zhang, B. Wang and X. H. Bao, *Science*, 2010, **328**, 1141.

20 (*a*) H. Boennemann and R. M. Richards, *Eur. J. Inorg. Chem.*, 2001, 2455; (*b*) C. Burda, X. Chen, R. Narayanan and M. A. El-Sayed, *Chem. Rev.*, 2005, **105**, 1025; (*c*) C. N. R. Rao, G. U. Kulkarni, P. J. Thomas and P. P. Edwards, *Chem. Soc. Rev.*, 2000, **29**, 27.

21 V. K. Lamer and R. H. Dinegar, *J. Am. Chem. Soc.*, 1950, **72**, 4847.

22 S. Marx and A. Baiker, *J. Phys. Chem. C*, 2009, **113**, 6191.

23 D. A. Handley, in *Colloidal Gold: Principles, Methods and Applications*, ed. M. A. Hayat, Academic, San Diego, CA, 1989.

24 L. Guczi, A. Beck, A. Horváth, Zs. Koppány, G. Stefler, K. Frey, I. Sajó, O. Geszti, D. Bazin and J. Lynch, *J. Mol. Catal. A: Chem.*, 2003, **204–205**, 545.

25 A. M. Venezia, L. F. Liotta, G. Pantaleo, V. La Parola, G. Deganello, A. Beck, Zs. Koppány, K. Frey, D. Horváth and L. Guczi, *Appl. Catal., A*, 2003, **251**, 359.

26 M. Sankar, N. Dimitratos, P. J. Miedziak, P. P. Wells, C. J. Kielye and G. J. Hutchings, *Chem. Soc. Rev.*, 2012, **41**, 8099.

27 (*a*) N. Dimitratos, F. Porta and L. Prati, *Appl. Catal., A*, 2005, **291**, 210; (*b*) C. L. Bianchi, P. Canton, N. Dimitratos, F. Porta and L. Prati, *Catal. Today*, 2005, **102–103**, 203; (*c*) M. Comotti, C. Della Pina and M. Rossi, *J. Mol. Catal. A: Chem.*, 2006, **251**, 89–92; (*d*) N. Dimitratos, C. Messi, F. Porta, L. Prati and A. Villa, *Appl. Catal., A*, 2006, **256**, 21; (*e*) N. K. Chaki, H. Tsunoyama, Y. Negishi, H. Sakurai and T. Tsukuda, *J. Phys. Chem. C*, 2007, **111**, 4885; (*f*) J. A. Lopez-Sanchez, N. Dimitratos, P. Miedziak, E. Ntainjua, J. E. Edwards, D. Morgan, A. F. Carley, R. Tiruvalam, C. J. Kiely and G. J. Hutchings, *Phys. Chem. Chem. Phys.*, 2008, **10**, 1921; (*g*) N. Dimitratos, J. A. Lopez-Sanchez, D. Morgan, A. F. Carley, R. Tiruvalam, C. J. Kiely, D. Bethell and G. J. Hutchings, *Phys. Chem. Chem. Phys.*, 2009, **11**, 5142; (*h*) J. Pritchard, L. Kesavan, M. Piccinini, Q. He, R. Tiruvalam, N. Dimitratos, J. A. Lopez-Sanchez, A. F. Carley, J. K. Edwards, C. J. Kiely and G. J. Hutchings, *Langmuir*, 2010, **26**, 16568.

28 R. C. Tiruvalam, J. C. Pritchard, N. Dimitratos, J. A. Lopez-Sanchez, J. K. Edwards, A. F. Carley, G. J. Hutchings and C. J. Kiley, *Faraday Discuss.*, 2011, **152**, 63.

29 D. Wang, A. Villa, F. Porta, D. Su and L. Prati, *Chem. Commun.*, 2006, 1956.

30 (*a*) A. Villa, C. Campione and L. Prati, *Catal. Lett.*, 2007, **115**, 133; (*b*) D. Wang, A. Villa, F. Porta, L. Prati and D. Su, *J. Phys. Chem. C*, 2008, **112**, 8617.

31 A. Villa, D. Wang, D. Su, G. M. Veith and L. Prati, *Phys. Chem. Chem. Phys.*, 2010, **12**, 2183.

32 (*a*) G. Li, D. I. Enache, J. Edwards, A. F. Carley, D. W. Knight and G. J. Hutchings, *Catal. Lett.*, 2006, **110**, 7; (*b*) D. I. Enache, D. Barker, J. K. Edwards, S. H. Taylor, D. W. Knight, A. F. Carley and G. J. Hutchings, *Catal. Today*, 2007, **122**, 407; (*c*) P. J. Miedziak, Z. Tang, T. E. Davies, D. I. Enache, J. K. Bartley, A. F. Carley, A. A. Herzig, C. J. Kiely, S. H. Taylor and G. J. Hutchings, *J. Mater. Chem.*, 2009, **19**, 8619.

33 G. J. Hutchings and C. J. Kiely, *Acc. Chem. Res.*, 2013, **46**, 1759.

34 A. Denton and N. Ashcroft, *Phys. Rev. A: At., Mol., Opt. Phys.*, 1991, **43**, 3161–3164.

35 H. M. Rietveld, *J. Appl. Crystallogr.*, 1969, **2**, 65–71.

36 A. Patterson, *Phys. Rev.*, 1939, **56**, 978–982.

37 B. W. Reed, D. G. Morgan, N. L. Okamoto, A. Kulkarni, B. C. Gates and N. D. Browning, *Ultramicroscopy*, 2009, **110**, 48–60.

38 A. Carlsson, A. Puig-Molina and T. V. W. Janssens, *J. Phys. Chem. B*, 2006, **110**, 5286–5293.

39 S. Hüfner, *Photoelectron Spectroscopy - Principles and Applications*, Springer, 2003.

40 A. A. Herzing, M. Watanabe, J. K. Edwards, M. Conte, Z.-R. Tang, G. J. Hutchings and C. J. Kiely, *Faraday Discuss.*, 2008, **138**, 337–351.

41 F. Liu, D. Wechsler and P. Zhang, *Chem. Phys. Lett.*, 2008, **461**, 254–259.

42 S. Nishimura, Y. Yakita, M. Katayama, K. Higashimine and K. Ebitani, *Catal. Sci. Technol.*, 2013, **3**, 351.

43 Y. Shi, H. Yang, X. Zhao, T. Cao, J. Chen, W. Zhu, Y. Yu and Z. Hou, *Catal. Commun.*, 2012, **18**, 142–146.

44 *X-ray Absorption: Principles, Applications, Techniques of EXAFS, SEXAFS, and XANES*, ed. D. C. Koningsberger and R. Prins, Wiley, 1987.

45 W. Ketchie, M. Murayama and R. Davis, *J. Catal.*, 2007, **250**, 264–273.

46 N. Tanaka, *Sci. Technol. Adv. Mater.*, 2008, **9**, 014111.

47 S. J. Pennycook and D. E. Jesson, *Ultramicroscopy*, 1991, **37**, 14–38.

48 M. Tsuji, K. Ikedo, M. Matsunaga and K. Uto, *CrystEngComm*, 2012, **14**, 3411.

49 P. Dash, T. Bond, C. Fowler, W. Hou, N. Coombs and R. W. J. Scott, *J. Phys. Chem. C*, 2009, **113**, 12719–12730.

50 M. Heggen, M. Oezaslan, L. Houben and P. Strasser, *J. Phys. Chem. C*, 2012, **116**, 19073–19083.

51 G. J. Hutchings, *Chem. Commun.*, 2008, 1148–1164.

52 H. Zhang and N. Toshima, *Catal. Sci. Technol.*, 2013, **3**, 268.

53 Q. He, P. J. Miedziak, L. Kesavan, N. Dimitratos, M. Sankar, J. A. Lopez-Sanchez, M. M. Forde, J. K. Edwards, D. W. Knight, S. H. Taylor, C. J. Kiely and G. J. Hutchings, *Faraday Discuss.*, 2013, **162**, 365.
54 D. Ferrer, A. Torres-Castro, X. Gao, S. Sepúlveda-Guzmán, U. Ortiz-Méndez and M. José-Yacamán, *Nano Lett.*, 2007, 7, 1701–1705.
55 D. Wang, A. Villa, P. Spontoni, D. S. Su and L. Prati, *Chem. – Eur. J.*, 2010, **16**, 10007–10013.
56 A. Villa, D. Wang, N. Dimitratos, D. Su, V. Trevisan and L. Prati, *Catal. Today*, 2010, **150**, 8.
57 A. Villa, N. Janjic, P. Spontoni, D. Wang, D. S. Su and L. Prati, *Appl. Catal., A*, 2009, **364**, 221.
58 D. Wang, A. Villa, P. Spontoni, D. S. Su and L. Prati, *Chem. – Eur. J.*, 2010, **16**, 10007.
59 J. A. Lopez-Sanchez, N. Dimitratos, N. Glanville, L. Kesavan, C. Hammond, J. K. Edwards, A. F. Carley, C. J. Kiely and G. J. Hutchings, *Appl. Catal., A*, 2011, **391**, 400.
60 Y. Hao, G.-P. Hao, D.-C. Guo, C.-Z. Guo, W.-C. Li, M.-R. Li and A.-H. Lu, *ChemCatChem*, 2012, **4**, 1595.
61 C. Y. Ma, B. J. Dou, J. J. Li, J. Cheng, Q. Hu, Z. P. Hao and S. Z. Qiao, *Appl. Catal., B*, 2009, **92**, 202.
62 Y. Chen, H. Wang, C.-J. Liu, Z. Zeng, H. Zhang, C. Zhou, X. Jia and Y. Yang, *J. Catal.*, 2012, **289**, 105.
63 C. Evangelisti, E. Schiavi, L. A. Aronica, A. M. Caporusso, G. Vitulli, L. Bertinetti, G. Martra, A. Balerna and S. Mobilio, *J. Catal.*, 2012, **286**, 224.
64 A. Villa, D. Wang, P. Spontoni, R. Arrigo, D. Su and L. Prati, *Catal. Today*, 2010, **157**, 89.
65 Y. Chen, H. Lim, Q. Tang, Y. Gao, T. Sun, Q. Yan and Y. Yang, *Appl. Catal., A*, 2010, **380**, 55.
66 L. Wang, W. Zhang, S. Zeng, D. Su, X. Meng and F. Xiao, *Chin. J. Chem.*, 2012, **30**, 2189.
67 M. Sankar, E. Nowicka, R. Tiruvalam, Q. He, S. H. Taylor, C. J. Kiely, D. Bethell, D. W. Knight and G. J. Hutchings, *Chem. – Eur. J.*, 2011, **17**, 6524.
68 A. Villa, D. Wang, G. M. Veith and L. Prati, *J. Catal.*, 2012, **292**, 73.
69 Q. He, P. J. Miedziak, L. Kesavan, N. Dimitratos, M. Sankar, J. A. Lopez-Sanchez, M. M. Forde, J. K. Edwards, D. W. Knight, S. H. Taylor, C. J. Kiely and G. J. Hutchings, *Faraday Discuss.*, 2013, **162**, 365.
70 A. Beck, A. Horvath, Z. Schay, Gy. Stefler, Zs. Koppany, I. Sajó, O. Geszti and L. Guczi, *Top. Catal.*, 2007, **44**, 115.
71 R. W. J. Scott, C. Sivadinarayana, O. M. Wilson, Z. Yan, D. W. Goodman and R. M. Crooks, *J. Am. Chem. Soc.*, 2005, **127**, 1380.
72 V. Abdelsayed, A. Aljarash and M. S. El-Shall, *Chem. Mater.*, 2009, **21**, 2825.
73 L. Delannoy, S. Giorgio, J. G. Mattei, C. R. Henry, N. El Kolli, C. Methivier and C. Louis, *ChemCatChem*, 2013, **5**, 2707.
74 M. Haruta, S. Tsubota, T. Kobayashi, H. Kageyama, M. J. Genet and B. Delmon, *J. Catal.*, 1993, **144**, 175.
75 F. Gao, Y. Wang and D. W. Goodman, *J. Phys. Chem. C*, 2010, **114**(9), 4036.
76 Z. Li, G. GaO and W. T. Tysoe, *J. Phys. Chem. C*, 2010, **114**, 16909.

